
Article:
Baldwin, Jack and Hancock, Yvette orcid.org/0000-0003-4799-2783 (2018) Role of random edge-disorder on the transport properties of ultra-thin zig-zag graphene nanoribbons. Journal of Physics: Conference Series. 012001. ISSN 1742-6596

https://doi.org/10.1088/1742-6596/964/1/012001

Role of random edge-disorder on the transport properties of ultra-thin zig-zag graphene nanoribbons

J P C Baldwin[1] and Y Hancock[1,2]

[1]Department of Physics, University of York, Heslington, York YO10 5DD, United Kingdom
[2]York Centre for Complex Systems Analysis, University of York, Heslington, York YO10 5GE, United Kingdom

E-mail: y.hancock@york.ac.uk

Abstract. We report on an introductory study used to gauge the significance of random weak-edge disorder on the coherent transport properties of ultra-thin zig-zag nanoribbons (ZGNRs) beyond the simple (*i.e.,* first nearest-neighbour) tight-binding approximation. Such extensions include up to third nearest-neighbour hopping in an extended tight-binding model, as well as a mean-field Hubbard-U. The effect of the random weak-edge disorder causes charge-carrier localization that reduces the conductance about the Fermi energy in all of the systems studied. In the non-interacting systems, the extended tight-binding model is found to be more robust against disorder due to the increased kinetic degrees of freedom. Localization effects from the random weak-edge disorder are found to compete with the mean-field Hubbard-U resulting in spin-dependent conductance properties.

1. Introduction

Edge roughness [1] and chemical disorder due to highly reactive edges [2] are common issues in the fabrication of graphene nanoribbons requiring realistic modelling and fast simulation for future device design. Within this context, the role of disorder on the transport properties of low-dimensional quantum systems becomes a key question, and thus, in this paper, we explore its effect in ultra-thin ZGNRs. Ideal ZGNRs are predicted to have antiferromagnetic order across the ribbon-width commensurate with Lieb's theorem for a half-filled bipartite lattice, and a band gap that varies inversely as a function of the increasing ribbon width [3]. With experimental measurements also showing magnetic signatures in graphene nanoribbons with ZGNR edges [4], the interplay between magnetic effects, system-dimension and random edge disorder becomes pertinent and timely considerations.

There are few density functional theory (DFT) studies on disordered ZGNRs most likely due to the computational cost involved in large unit cell calculations. One such study by Huang *et al.* on ZGNRs with *systematic* edge-vacancy defects predicted a loss of magnetism at 33% edge-vacancy concentration [5]. Using a generalized tight-binding (GTB) model with mean-field Hubbard-U that reproduces DFT trends, we were able to verify that the loss of magnetism in the systematic study was due to finite size effects [6]. When *random* edge-vacancy disorder was considered within ensemble-averaging in ultra-thin ZGNRs, our results showed a persistent magnetic state and onset of spin-dependent transport for increasing ribbon length, indicating the dominance of the magnetic interaction against disorder.

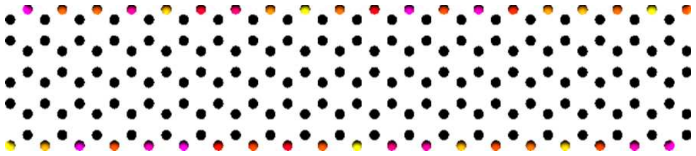

Figure 1. A section of an ultra-thin, 5-atom-wide (9.24 Å) ZGNR device studied in this work. The coloured edge-atoms have weak-disorder implemented by the random perturbation of the site-dependent on-site energy $\epsilon_{i(edge)}$ within the range V=±0.5 eV as applied through the Hamiltonian in Eq. 1. Various system lengths are investigated: 73.8, 86.1, 123.0 and 147.6 Å.

Most tight-binding transport studies on disordered graphene nanoribbons use a non-interacting nearest neighbour (*i.e.,* simple) tight-binding model (STB). For example, Refs. [7, 8]. Here, we extend this work and our previous studies on random edge-vacancy disorder [6], to investigate weak-edge disorder introduced by random perturbation to the local edge-atom chemical potentials in ultra-thin ZGNRs (Fig. 1). Other published studies that use the STB model show ZGNRs to be less robust against this type of disorder compared to armchair graphene nanoribbons (AGNRS), with these systems also having a transport gap that opens due to Anderson localization [7, 8]. By investigating the effect of random weak-edge disorder beyond the STB approximation, we will test the interplay of increased kinetics using an extended tight-binding (ETB) model (up to third nearest neighbour), and interaction effects by applying a generalized tight binding (GTB) model with mean-field Hubbard-U.

2. Theory and computational method

The GTB Hamiltonian is defined as

$$H = \sum_{i\sigma} \epsilon_i n_{i\sigma} n_{i\sigma} - \sum_{ij\sigma} (t_{ij} c^{\dagger}_{i\sigma} c_{j\sigma} + H.c.) + \sum_{i} U n_{i\sigma} n_{i-\sigma} \tag{1}$$

where $c^{\dagger}_{i\sigma}(c_{j\sigma})$ is the fermion creation (destruction) operator, which creates (destroys) an electron with spin $\sigma = \{\uparrow, \downarrow\}$ at site i (j), $n_{i\sigma} = 1$ or 0 is the spin-dependent number operator, and *H.c.* is the Hermitian conjugate. The model is parameterised using the parameter set in Ref. [9], where U = 2.0 eV denotes the Hubbard-U (*i.e.,* the local Coulomb interaction energy between opposite spins [10]), and t_{ij} are the hopping energies equal to 2.7 eV, 0.20 eV and 0.18 eV for first, second and third nearest neighbor hopping, respectively. To model random weak-edge disorder, the local on-site energy of each edge atom $\epsilon_{i(edge)}$ has been randomly perturbed in the range V = ±0.5 eV (Fig. 1). To solve the Hamiltonian, a mean-field approximation is used maintaining a half-filled system, where

$$n_{i\sigma} n_{i-\sigma} = \langle n_{i\sigma} \rangle n_{i-\sigma} + n_{i\sigma} \langle n_{i-\sigma} \rangle - \langle n_{i\sigma} \rangle \langle n_{i-\sigma} \rangle \tag{2}$$

and $\langle n_{i\sigma} \rangle$ is the expectation associated with the local spin-occupancy. Using this approximation, Eq. (1) can be decoupled and linerarized into two spin-dependent Hamiltonians, which are then solved self-consistently. For further details about the self-consistent method see Ref. [11].

The coherent transport properties of the ZGNRs are calculated using the Landauer-Bütticker formalism [12] assuming that the device has semi-infinite ZGNR leads. The spin-dependent conductance $\mathrm{G}_{\sigma}(E)$ at energy E is determined from the transmission function $T_{\sigma}(E)$, such that,

$$\mathrm{G}_{\sigma}(E) = \frac{e^2}{h} T_{\sigma}(E) \tag{3}$$

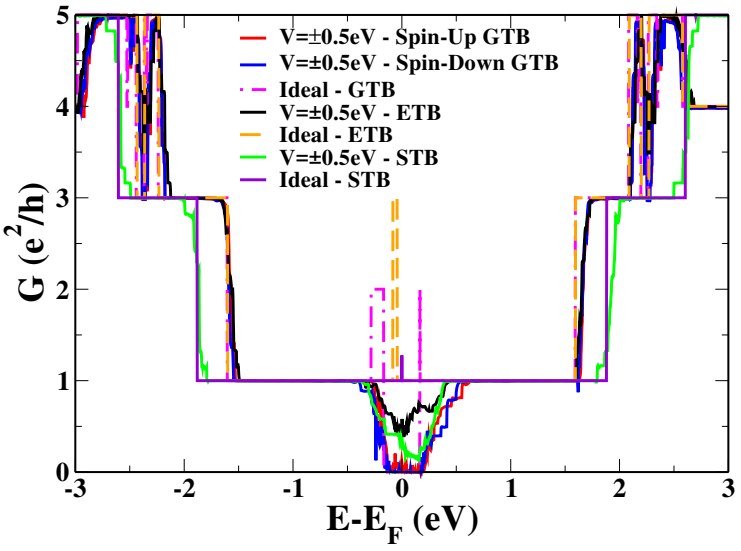

Figure 2. The ensemble-averaged conductance G in units of the quantum conductance (e^2/h) versus the energy E relative to the Fermi energy E_F for ideal and random weak-edge-disordered STB, ETB and GTB systems measured in the range -3 eV $\leq E - E_F \leq 3$ eV. The local on-site potential is randomly varied in the range $V = \pm 0.5$ eV. The systems have a device length of 146.7 Å. For the GTB results, both spin-channels are shown.

where

$$T_\sigma(E) = \mathrm{Tr}[\Gamma_{L\sigma}(E)\mathrm{G}_\sigma^{Ret}(E)\Gamma_{R\sigma}(E)\mathrm{G}_\sigma^{Adv}(E)] \tag{4}$$

and $\mathrm{G}_\sigma^{Ret/Adv}(E)$ are the retarded/advanced Green's functions. The $\Gamma_{L/R\sigma}(E)$ matrices are calculated from

$$\Gamma_{L/R\sigma}(E) = [\Sigma_{L/R\sigma}^{Ret}(E) - \Sigma_{L/R\sigma}^{Adv}(E)] \tag{5}$$

where

$$\Sigma_{L/R\sigma}^{Ret/Adv}(E) = V_{L/R}^\dagger g_{L/R\sigma}^{Ret/Adv}(E) V_{L/R}. \tag{6}$$

Here, $V_{L/R}$ describes the coupling between the ZGNR device and the L/R lead, and $g_{L/R\sigma}^{Ret/Adv}(E)$ are the retarded/advanced surface Green's functions for the leads, which have been obtained using the decimation iteration method [13]. The transmission function is calculated using the methods described in Ref. [14]. Our application of this formalism was tested against density functional theory transport results in Hancock *et al.* 2010 [9], and also applied in other works, such as Baldwin and Hancock 2016 [6]. To calculate the effect of random edge-disorder, an ensemble average is obtained where $\chi \approx \bar{x} = \frac{1}{N}\sum_{i=1}^{N} x_i$. Here, $\bar{x}$ is the average value of a calculated property taken over the sample size, N, x_i is the measured property for the *ith* system in the ensemble population, and χ is the ensemble average. The standard error (SE) associated with the ensemble average is $\mathrm{SE} = \frac{\sigma}{\sqrt{N}}$ where σ is the standard deviation.

3. Results & Discussion

Figure 2 shows the ensemble-averaged conductance for the disordered and ideal STB, ETB and GTB systems as a function of the energy E relative to the Fermi energy E_F. A device length of 146.7 Å was chosen as longer devices are more susceptible to disorder due to the expected decrease in conductance arising from increased charge-carrier localization. To determine the number of randomly-defected systems (N) in each ensemble that are needed to obtain these

results, a convergence test was performed for the ensemble-averaged conductance measured at the Fermi energy G_{E_F} in the STB, ETB and GTB calculations. In performing this test, a strict convergence criterion was set such that the ensemble-averaged results were deemed converged when $G_{E_F}[N] - G_{E_F}[N-1] \leq 0.01\ e^2/h$. Application of this criterion resulted in convergence of the transport results at N=24 for the non-interacting STB and ETB systems, and at N=12 for the GTB spin-up and spin-down solutions. The smaller number of N=12 systems required to converge the ensemble-average GTB transport results, compared to N=24 for the ETB and STB solutions, indicates the stabilizing effect of the mean-field Hubbard-U against disorder.

The ensemble-averaged transport results show a reduced conductance for the disordered systems, particularly about E_F, compared to the results for the ideal devices (Fig. 2). In the non-interacting results, the ETB system is found to be more robust to disorder compared to the STB system due to the increased kinetic degrees of freedom in the former, with both systems exhibiting perturbations to the conduction up to the second conduction step. Although the conduction is reduced at E_F for the disordered STB and ETB systems, it remains finite (hence statistically significant) against the calculated standard error (SE) (Table 1)—*i.e.,* these results are greater in magnitude than the $0.01{*}e^2/h$ threshold established for experimental validity [1].

The ensemble-averaged GTB results for the interacting disordered system show a break-down in the Hubbard-U gap when compared to the ideal GTB solutions (Fig. 2). A finite conductance is determined for the spin-up channel, and a zero conductance for the spin-down channel at E_F against the SE and the $0.01{*}e^2/h$ criterion (Table 1). The asymmetry of the disorder across the ribbon-width is the underlying cause of these spin-dependent results. The unequal local chemical potentials on the device edge-atoms obtained through the random edge-disorder, as well as at the lead connections, perturb the magnetic state and transport leading to a finite spin-dependent conduction within the Hubbard-U gap region in the GTB solutions.

Table 1. Ensemble-averaged G_{E_F} and associated standard error (SE) for the disordered systems.

System	G_{E_F} (e^2/h)	SE (e^2/h)	$G_{E_F} \pm$ SE (e^2/h)
STB	0.23	0.09	0.14 to 0.32
ETB	0.5	0.1	0.4 to 0.6
GTB (spin-up channel)	0.05	0.02	0.03 to 0.07
GTB (spin-down channel)	8E-5	3E-5	5E-5 to 1.1E-4

To determine the effect of charge carrier localization due to disorder, the conductance at E_F is plotted as a function of the system length (Fig. 3). At a given energy E, the localization length ζ can be obtained from

$$G(L) = G_0(L)e^{\frac{-L}{\zeta}}, \tag{7}$$

where G is the conductance in the disordered system, G_0 is the conductance of the ideal system and L is the length of the device [15]. Using this equation, and from the exponential fits to the results in Fig. 3, the localization lengths have been determined as 65 Å for the STB system and 101 Å for the ETB system, both with ∼30% uncertainty, meaning that the charge-carriers are well-localized in the previously studied device length of 146.7 Å. The STB results are found to be in good agreement compared to ensemble-averaged STB results on similarly disordered systems [7], and as expected, the ETB localization length is longer than the STB localization length due to the increased kinetic degrees of freedom in the former. At longer device lengths and/or for higher maximum values of the disorder strength $|V|$, a disorder gap is expected that

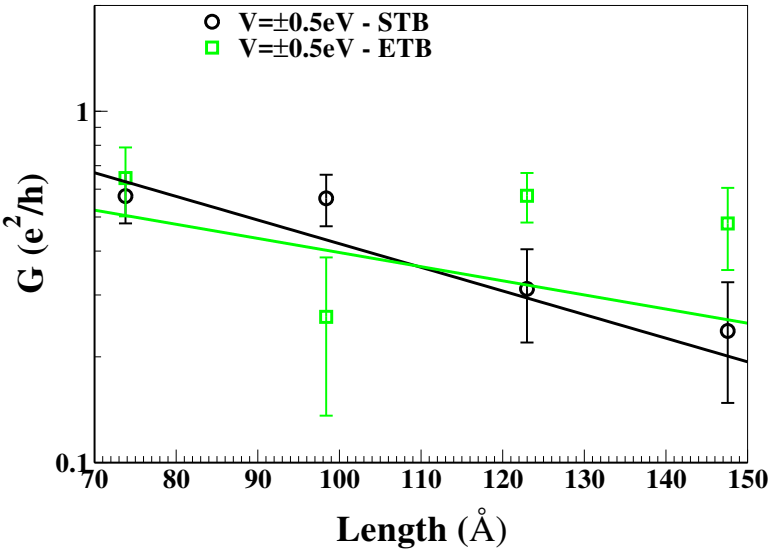

Figure 3. The ensemble-averaged conductance G measured at the Fermi energy E_F in units of quantum conductance (e^2/h) versus system length for the STB and ETB random edge-disordered systems. The local on-site potential is randomly varied in the range $V = \pm 0.5$ eV. Using exponential fitting, the localization lengths are determined as 65 Å for the STB system and 101 Å for the ETB system, both with ∼30% uncertainty. The error bars correspond to ± the standard error (SE).

will influence these findings, as well as begin to compete with the Hubbard gap in the GTB results, with the study of these effects being the topic of future work.

4. Conclusion

An introductory study has been performed to gauge the significance of random weak-edge disorder on the coherent transport properties of ultra-thin ZGNRs beyond the simple (*i.e.,* first nearest-neighbour) tight-binding (STB) model. These extensions have included up to third nearest-neighbour hopping in an extended tight-binding (ETB) model, as well as a mean-field Hubbard-U interaction (GTB model). Within ensemble averaging, the effect of the disorder causes charge-carrier localization reducing the STB, ETB and GTB conductances, with the ETB system being more robust relative to the STB due to increased kinetic degrees of freedom. Faster convergence of the ensemble-averaged transport relative to the ensemble size for the GTB also indicates the stabilizing effect of the mean-field Hubbard-U. Asymmetric edge-disorder and connection to the leads results in spin-dependent perturbations that reduce the effective Hubbard-U causing single spin-channel conductance at the Fermi energy. Further studies will involve testing a range of on-site energy disorder strengths and device dimensions.

Acknowledgments

This work made use of the facilities of the N8 HPC Centre of Excellence, provided and funded by the N8 Consortium and EPSRC (United Kingdom), EP/K000225/1. We also acknowledge the University of York's award of a dedicated cluster (Nano) to YH's research group for theoretical graphene research. An EPSRC (United Kingdom), EP/P505798/1, PhD studentship was awarded to YH from the Department of Physics for JPCB. All data created during this research are available by request from the University of York Data Catalogue http://dx.doi.org/10.15124/ea325b7b-c4ed-4bbf-9c4a-0de6e8c0cbba.

References

[1] Han M Y, Özyilmaz B, Zhang Y and Kim P 2007 *Physical Review Letters* **98**, 206805
[2] Allen M J, Tung V C and Kaner R B 2010 *Chemical Reviews* **110**, 132
[3] Son Y -W, Cohen M L, and Louie S G 2006 *Physical Review Letters* **97**, 216803
[4] Tao C, Jiao L, Yazyev O V, Chen Y -C, Feng J, Zhang X, Capaz RB, Tour J M, Zettl A, Louie S G, Dai H and Crommie M F 2011 *Nature Physics* **7**, 616
[5] Huang B, Liu F, Wu J, Gu B -L and Duan W 2008 *Physical Review B* **77** 153411
[6] Baldwin J P C and Hancock Y 2016 *Physical Review B* **94**, 165126
[7] Li T C and Lu S -P 2008 *Physical Review B* **77**, 085408
[8] Cresti A, Nemec N, Biel B, Niebler G, Triozon F, Cuniberti G, and Roche S 2008 *Nano Research* **1**, 361
[9] Hancock Y, Uppstu A, Saloriutta, K, Harju A and Puska M J 2010 *Physical Review B* **81**, 245402
[10] Hubbard J 1963 *Proceedings of the Royal Society (London) Series A* **276**, 238
[11] Hancock Y and Smith A E 2003 *Physica E* **18** 383
[12] Datta S 1997 *Electronic Transport in Mesoscopic Systems* Cambridge University Press, Cambridge, U.K.
[13] Guinea F, Tejedor C, Flores F, and Louis E 1983 *Physical Review B* **28**, 4397
[14] Muñoz-Rojas F, Jacob D, Fernández-Rossier J and Palacios J 2006 *Physical Review B* **74**, 195417
[15] Beenakker C W J 1997 *Reviews of Modern Physics* **69** 731